CFSRC COLLOQUIUM

*Proceedings of the Cold-Formed Steel Research Consortium Colloquium*
*20-22 October 2020 (cfsrc.org)*

# Prediction model of Power-Actuated Fasteners subjected to pull-out from Cold-formed steel plates

An Nhien Truong[1], Cao Hung Pham[2], Gregory J. Hancock[3]

## Abstract

An experimental program comprising of sixty-nine cross-tension test specimens was carried out to investigate the pull-out behaviour of Power-Actuated Fastener (PAF) connections joining two cold-formed steel (CFS) plates under quasi-static monotonic tensile loading. The studied parameters were the diameter of the fasteners and the thicknesses of the top and base steel plates. The fasteners had diameters of 3.7 mm, 4.5 mm, and 4.0 mm, from two manufacturers Hilti Pty Ltd. and Ramset$^{TM}$. The top sheets had thicknesses ranging from 1.5 to 4.0 mm and the base plates had thicknesses ranging from 3.0 to 20.0 mm. The test results reveal that PAF connections exhibit a high pull-out capacity providing sufficient embedment length is provided. A model is proposed to evaluate the pull-out strength of the PAF connections based on the base material strength, the diameter and embedment length of the fastener. The equation proposed in the model produces a test-to-prediction mean ratio of 1.02 with a coefficient of variation of 0.12.

## 1. General

Power-Actuated Fastening is a technique which uses a powder cartridge or compressed gas as the energy source to drive a hardened fastener directly into the base material. In steel construction, Power-Actuated Fasteners (PAFs) can be used in conjunction with bolts and screws to boost the speed of construction process while ensuring in the safety and reliability. Recently, a design provision for PAF in Cold-formed steel (CFS) connections has been adopted to North American Specification AISI S100:2016 [1] and Australian Standard AS/NZS 4600:2018 [2]. This provision provides design guidelines for various limit states when the connections are subjected to shear or tensile loading. However, there is no equation to predict the pull-out strength of the PAF connections under tension due to the complexity of the anchoring mechanisms which hold the fastener in place and the diversity of PAFs in terms of geometric features and metallurgical properties [3]. The design standard and specification recommend that the pull-out strength of PAF connections should be determined by testing or should rely upon the information provided by the manufacturers [4, 5]. Therefore, it is necessary to develop a generic model to be incorporated into the design standard and specification based on sufficient testing data. Experimental studies into the shear behaviour of PAFs in the connections of steel tubular sections, shear ribs in steel decking, and steel diaphragms were conducted by Kosteski et al., Fontana and Beck, and Roger and Trembley, respectively [6, 7, 8]. Meanwhile, the majority of experimental studies into the behaviour of PAFs under tension were done by the manufacturers which are unpublished or inaccessible.

In this study, an experimental program comprised of sixty-nine (69) specimens, corresponding to 23 configurations, were tested under quasi-static monotonic loading. Based on the test results, a generic model is proposed to predict the pull-out strength of the PAF connections under tension. The proposed model utilizes various deterministic parameters i.e. the strength of base plate, geometry, and embedded length of the fastener. For the unknown factors such as the unique features of the PAF and reactionary force, they are also considered by three coefficients which are calibrated from the test results.

[1] Doctoral Candidate, School of Civil Engineering, The University of Sydney, Sydney, New South Wales, NSW 2006, Australia. Email: annhien.truong@sydney.edu.au
[2] Senior Lecturer in Structural Engineering, School of Civil Engineering, The University of Sydney, Sydney, New South Wales, NSW 2006, Australia. Email: caohung.pham@sydney.edu.au
[3] Professorial Research Fellow and Emeritus Professor, School of Civil Engineering, The University of Sydney, Sydney, New South Wales, NSW 2006, Australia. Email: gregory.hancock@sydney.edu.au

## 2. Experimental program

### *2.1 Material properties*

Table 1 shows the design parameters of the specimens and their measured material properties. In the nomenclature of each specimen, the first number denotes the specified diameter of the PAF used, the second number denotes the thickness of the top sheet ($t_1$), and the last number denotes the thickness of the base plate ($t_2$). For instance, 4.5-3.0-6.0 means that a PAF with a diameter of 4.5 mm is used to connection a thin sheet of 3.0 mm to a thicker sheet of 6.0 mm. It is noted that this study focuses on the pull-out limit state; therefore, the other limit states of PAF connections subjected to tension (i.e. pull through of top sheet or pull-over of washer) is not included.

Table 1. Properties of the test specimens

| Specimen | PAF | Top steel sheet | | | Base steel sheet | | |
|---|---|---|---|---|---|---|---|
| | $d_s$ (mm) | $t_1$ (mm) | $f_{y1}$ (MPa) | $f_{u1}$ (MPa) | $t_2$ (mm) | $f_{y2}$ (MPa) | $f_{u2}$ (MPa) |
| 3.7-2.4-3.0 | 3.7 | 2.4 | 557 | 589 | 3.0 | 531 | 558 |
| 3.7-2.4-4.0 | 3.7 | 2.4 | 557 | 589 | 4.0 | 422 | 497 |
| 3.7-3.0-4.0 | 3.7 | 3.0 | 531 | 558 | 4.0 | 422 | 497 |
| 3.7-2.4-6.0 | 3.7 | 2.4 | 557 | 589 | 6.0 | 576 | 639 |
| 3.7-3.0-6.0 | 3.7 | 3.0 | 531 | 558 | 6.0 | 576 | 639 |
| 3.7-4.0-6.0 | 3.7 | 4.0 | 422 | 497 | 6.0 | 576 | 639 |
| 4.5-2.4-3.0 | 4.5 | 2.4 | 557 | 589 | 3.0 | 531 | 558 |
| 4.5-2.4-4.0 | 4.5 | 2.4 | 557 | 589 | 4.0 | 422 | 497 |
| 4.5-3.0-4.0 | 4.5 | 3.0 | 531 | 558 | 4.0 | 422 | 497 |
| 4.5-2.4-6.0 | 4.5 | 2.4 | 557 | 589 | 6.0 | 576 | 639 |
| 4.5-3.0-6.0 | 4.5 | 3.0 | 531 | 558 | 6.0 | 576 | 639 |
| 4.5-4.0-6.0 | 4.5 | 4.0 | 422 | 497 | 6.0 | 576 | 639 |
| 4.5-2.4-9.0 | 4.5 | 2.4 | 557 | 589 | 9.0 | 618 | 691 |
| 4.5-3.0-9.0 | 4.5 | 3.0 | 531 | 558 | 9.0 | 618 | 691 |
| 4.5-4.0-9.0 | 4.5 | 4.0 | 422 | 497 | 9.0 | 618 | 691 |
| 4.5-3.0-20.0 | 4.5 | 3.0 | 531 | 558 | 20.0 | 335 | 469 |
| 4.0-1.5-3.0 | 4.0 | 1.5 | 603 | 622 | 3.0 | 531 | 558 |
| 4.0-2.4-3.0 | 4.0 | 2.4 | 557 | 589 | 3.0 | 531 | 558 |
| 4.0-1.5-4.0 | 4.0 | 1.5 | 603 | 622 | 4.0 | 422 | 497 |
| 4.0-1.5-6.0 | 4.0 | 1.5 | 603 | 622 | 6.0 | 576 | 639 |
| 4.0-2.4-6.0 | 4.0 | 2.4 | 557 | 589 | 6.0 | 576 | 639 |
| 4.0-3.0-6.0 | 4.0 | 3.0 | 531 | 558 | 6.0 | 576 | 639 |
| 4.0-4.0-6.0 | 4.0 | 4.0 | 422 | 497 | 6.0 | 576 | 639 |

Three different types of PAFs were used in this study. They were HILTI ENP2K-20L15, HILTI ENP-19L15, and RAMSET SBR9 with diameters of 3.7 mm, 4.5 mm, and 4.0 mm, respectively, from two manufacturers Hilti Pty Ltd and Ramset™. They are made from high-strength steel with the yield strength of approximately 1822 MPa. The Power-Actuator Tools used to drive the fastener into the steel materials are DX 76 (for HILTI ENP2K-20L15 and HILTI ENP-19L15) and RAMSET FormMaster (for RAMSET SBR9). The photos of the tools and PAFs are illustrated in Figure 1.

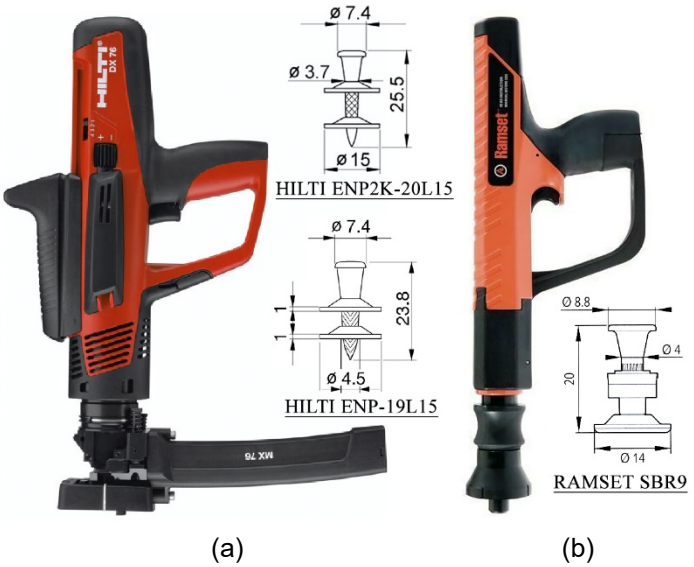


Figure 1. Power-Actuator Tools and fasteners from the manufacturers of (a) HILTI Pty LTd. and (b) RAMSET™ [4, 5]

Regarding the material properties, the steel sheets with thicknesses of 1.5-3.0 mm are cold-reduced sheet steel to AS 1397:2011 [9]. The sheets with the thickness of 4.0 mm were cut from Grade C450L0 equal angles L75x75x4.0 CA. The plates with the thicknesses of 6.0 and 9.0 were cut from Grade C450L0 rectangular hollow sections to AS/NZS 1163:2016 [10]. For the thickness of 20 mm, the material was hot-rolled steel to AS/NZS 3678:2016 [11].

### *2.2 Test setup*

To investigate the pull-out strength of the PAF connections under tension, cross-tension tests were conducted as per Appendix F4 of AS/NZS 4600:2018 [2]. The specimen was made from two steel sheets being joined by a PAF at the center of the overlapped area to form a cross (Figure 2). In each specimen, the base plate was always thicker than the top sheet in order to minimise the deformation of the steel sheets caused by the dynamic impact which occurred when the fastener was being fired. After the specimen was fabricated, it was assembled to the holding jigs in an upside down position. During the test, the upper holding jig connected to the base plate was fixed to the upper collet gripper which did not move whereas the lower holding jig connected to the top sheet was pulled as the lower collet

gripper of the testing machine moving downward. Figure 2 illustrates a typical test setup. The experiments were conducted using an 810 MTS servo-hydraulic testing machine in the J.W. Roderick Laboratory for Materials and Structures at the University of Sydney. The displacements were captured by two pairs of Linear Variable Differential Transformers (LVDTs) which were placed on the two sides of the upper and lower holding jigs as illustrated in Figure 2. Monotonic tensile loading was applied using displacement-control at a slow speed of 0.5-1.0 mm/min. The tests were terminated when the tensile force dropped to zero due to the pull-out of the fastener.

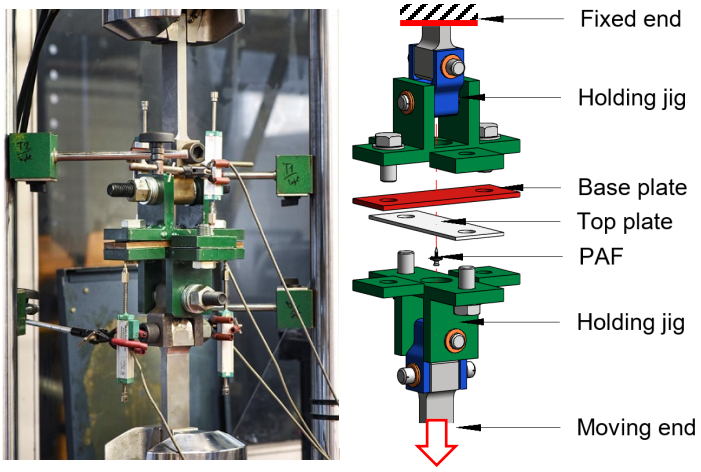


Figure 2. A typical test setup

## 3. Test results and Discussions

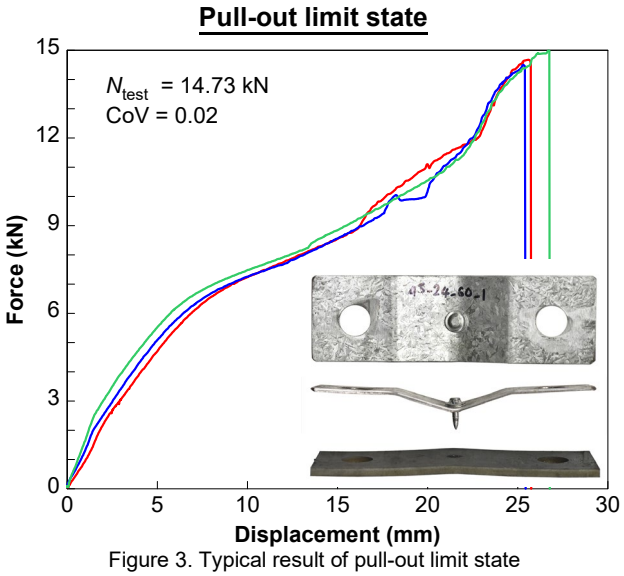


Figure 3. Typical result of pull-out limit state

Figure 3 illustrates a typical force-displacement characteristic and damage condition of the connectors of a PAF connection which failed in the pull-out limit state. It can be seen that after the peak load was reached, the tension force dropped in a non-ductile manner as the fastener was pulled out of the base material. The test results of all pull-out tests are set out in Table 2. For each configuration, three tests were conducted for reliability. The maximum COV of 8% indicates the consistency of the pull-out tests.

Table 2. The results of pull-out tests

| Specimen | Test results | | | | |
|---|---|---|---|---|---|
| | $N_{test\_1}$ (kN) | $N_{test\_2}$ (kN) | $N_{test\_3}$ (kN) | $N_{test}$ (kN) | COV |
| 3.7-2.4-3.0 | 7.80 | 8.55 | 8.62 | 8.32 | 0.04 |
| 3.7-2.4-4.0 | 11.15 | 10.92 | 10.23 | 10.77 | 0.04 |
| 3.7-3.0-4.0 | 11.43 | 11.50 | 11.52 | 11.48 | 0.003 |
| 3.7-2.4-6.0 | 17.05 | 15.87 | 17.42 | 16.78 | 0.04 |
| 3.7-3.0-6.0 | 12.96 | 14.77 | 13.54 | 13.76 | 0.05 |
| 3.7-4.0-6.0 | 11.52 | 9.85 | 10.01 | 10.46 | 0.07 |
| 4.5-2.4-3.0 | 9.57 | 9.81 | 10.28 | 9.89 | 0.03 |
| 4.5-2.4-4.0 | 13.26 | 12.83 | 13.31 | 13.13 | 0.02 |
| 4.5-3.0-4.0 | 12.21 | 13.02 | 12.61 | 12.61 | 0.03 |
| 4.5-1.5-6.0 | 14.62 | 14.59 | 14.28 | 14.50 | 0.01 |
| 4.5-2.4-6.0 | 14.68 | 14.51 | 15.00 | 14.73 | 0.01 |
| 4.5-3.0-6.0 | 12.18 | 14.13 | 12.98 | 13.10 | 0.06 |
| 4.5-4.0-6.0 | 12.49 | 12.02 | 12.24 | 12.25 | 0.02 |
| 4.5-2.4-9.0 | 14.31 | 13.12 | 14.36 | 13.93 | 0.04 |
| 4.5-3.0-9.0 | 11.52 | 11.51 | 13.12 | 12.05 | 0.06 |
| 4.5-4.0-9.0 | 9.55 | 10.24 | 11.10 | 10.30 | 0.06 |
| 4.5-3.0-20.0 | 14.74 | 15.99 | 17.36 | 16.03 | 0.08 |
| 4.0-1.5-3.0 | 8.01 | 8.72 | 8.18 | 8.30 | 0.04 |
| 4.0-2.4-3.0 | 8.29 | 8.47 | 8.62 | 8.46 | 0.02 |
| 4.0-1.5-4.0 | 11.50 | 10.00 | 10.60 | 10.70 | 0.06 |
| 4.0-1.5-6.0 | 11.55 | 11.73 | 11.31 | 11.53 | 0.01 |
| 4.0-2.4-6.0 | 11.62 | 10.67 | 13.05 | 11.78 | 0.08 |
| 4.0-3.0-6.0 | 10.60 | 9.40 | 11.43 | 10.48 | 0.08 |
| 4.0-4.0-6.0 | 8.75 | 9.22 | 8.06 | 8.68 | 0.05 |

According to previous studies into the anchorage mechanism of PAF in steel connection, it was revealed that when a fastener has been driven into the base steel material, four mechanisms namely clamping, fusion, soldering, and mechanical interlock, may act simultaneously to hold the fastener in place through friction [4]. Therefore, the pull-out capacity of a PAF connection may be related to the base material strength, the area of contact which is defined by the diameter of the PAF and the embedment length, and the knurling pattern on the PAF body.

From Table 2, the test data was extracted to demonstrate the influence of the thickness of the base plate ($t_2$) and the top sheet ($t_1$) on the maximum pull-out capacity in shown in Figures 4(a) and (b), respectively. It can be seen that the thickness of the base plate has a positive correlation with the pull-out capacity. For all of fastener types, the pull-out capacity increased when the base steel thickness increased from 2.4 to 6.0 mm owing to the increase in the contact area between the base steel plate and the embedded PAF body. However, when the thickness of the base plate increased to 9.00 mm, the pull-out capacity of the HILTI ENP-19L15 fastener ($d_s$ = 4.5 mm) decreased slightly by 6%. This reduction of strength was caused by the deformed steel material which exerted a stress in the direction normal to the surface at the fastener point and caused a reactionary force which pushed the fastener out of the base material (Figure 5). In Figure 4(b), it can be seen that the pull-out capacity decreased consistently as the thickness of the top steel sheet increased because the thick top sheet hindered the penetration capability of the PAF into the base material and resulted in a decrease of embedment length which eventually led to a drop of pull-out capacity. The influence of PAF geometric features can also be observed in Figure 4. The diameter of PAF has a direct influence on the pull-out capacity; however, it is not as significant as the PAF length. For example, regardless of the smaller diameter of 3.7 mm, the HILTI ENP2K-20L15 had the advantage in length in comparison with the other types (Figure 1). It allowed the HILTI ENP2K-20L15 specimens to have a higher pull-out strength than that of the RAMSET SBR9 fastener which was much shorter.

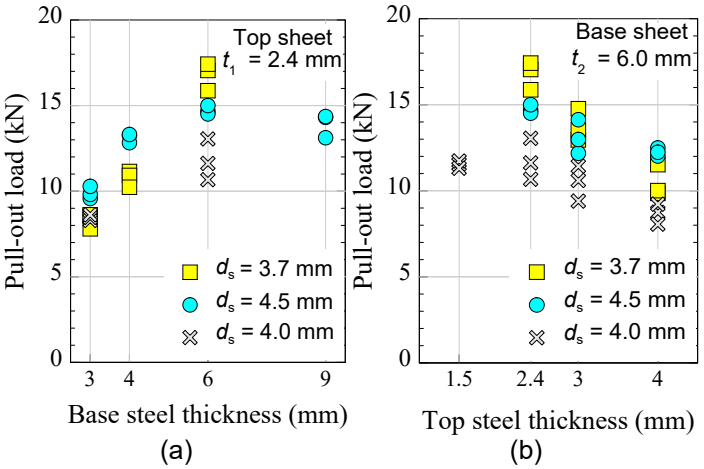


Figure 4. Influence of base plate and top sheet thickness on pull-out capacity

It is to be noted that the PAFs used in this study were specifically designed for steel connections. As illustrated in Figure 1, HILTI ENP-19L15 and RAMSET SBR9 fasteners have knurling patterns on the shank and the point; and HILTI ENP2K-20L15 fastener has a knurling pattern on the shank. According to a previous study (HILTI 2018), the presence of knurling has a remarkable influence on the pull-out strength i.e. the fasteners with a knurled body may possess 50% higher pull-out capacity than that with a smooth body.

## 4. Prediction model for pull-out strength

Based on the observations in Section 3, it is clear that the critical parameters which influence the pull-out capacity of PAF connections subjected to tension are the characteristics of the base steel plate, the embedment length, and the geometric features of the fastener. Cases in which any part of the PAF point is embedded in the base material, the reactionary force should be considered because it has a detrimental influence on the pull-out capacity. It is proposed in this paper that the pull-out capacity of PAF connections under tension, $N_{not}$, is the holding force of the PAF body embedded in the base material, $N_{hold}$, subtracting the reactionary force, $N_{react}$ (if present). The proposed model is presented in Figure 5 and Equation 1 where the total holding force is the summation of the holding force along the PAF shank, $N_{shank}$, and PAF point, $N_{point}$, which can be calculated as per Equations 1a and 1b. Meanwhile, the reactionary force, $N_{react}$, can be computed as per Equation 1c.

$$N_{not} = N_{hold} - N_{react} = \left(N_{shank} + N_{point}\right) - N_{react} \quad (1)$$

$$\text{where } N_{shank} = \alpha_1 \left(0.6 f_{u2}\right)\left(\pi d_{s1}\right) l_1 \quad (1a)$$

$$N_{point} = \alpha_2 \left(0.6 f_{u2}\right) \pi \left(\frac{d_{s1} + d_{s2}}{2}\right) l_2 \quad (1b)$$

$$N_{react} = \alpha_3 f_{y2} \pi \left(\frac{d_{s1} + d_{s2}}{2}\right) l_2 \quad (1c)$$

$$l_e = L_{fastener} - \text{NHS} - t_1 = l_1 + l_2 \quad (2)$$

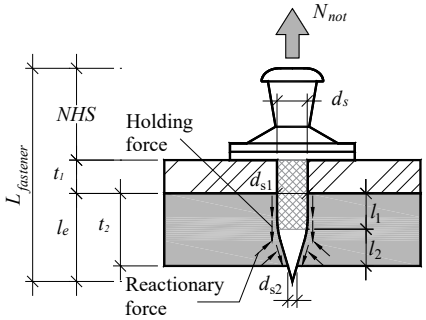


Figure 5. Proposed pull-out model

Depending on the length of the fastener and the thickness of the top sheet and base plate, three scenarios of embedment can occur as illustrated in Figure 6. Figure 6(a) illustrates the No Penetration case where the PAF body (including the shank and the point) is fully embedded in the base material. In this case, the embedment length, $l_e$, defined as the distance from the top surface of the base steel material to the tip of the fastener, can be calculated by

subtracting the nail head stand-off (NHS) and the thickness of the top sheet ($t_1$) from the total length of the fastener ($L_{\text{fastener}}$) as in Equation 2. For the cases of Partial Penetration and Full Penetration as illustrated in Figures 6(b) and (c), respectively, when the tip of the fastener can penetrate the base material and is visible on the other side, the embedment length is limited by the summation of the embedded length of the shank and the point of the fastener in the base material, $l_1$ and $l_2$, respectively. For simplification, it is assumed that within the length of the fastener shank, the nominal diameter, $d_s$, is unchanged and within the length of the fastener point, the diameter decreases linearly to zero as shown in Figure 1. Besides, it is assumed that protuberance is not present, and the deformation of the steel plates is negligible. These assumptions allow the values of the diameters of the fastener at the near side and far side of the base material, $d_{s1}$ and $d_{s2}$, to be estimated diagrammatically as shown in Figure 6 based on the fastener geometry and its embedded length in the base material.

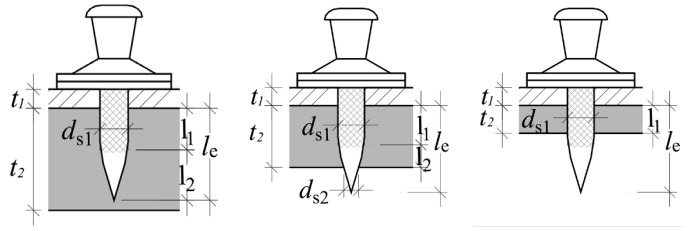

Figure 6. Three pull-out cases of the proposed model (a) No Penetration; (b) Partial Penetration; and (c) Full Penetration

In the light of the diversity of commercially available PAFs, two coefficients $\alpha_1$ and $\alpha_2$ are introduced to account for the unique features [i.e., geometric features, metallurgical properties of the fasteners, or knurling patterns (if present)] at the shank and the point of each type of fastener, respectively. Meanwhile, the coefficient $\alpha_3$ is introduced to account for the reactionary force (if present). These three coefficients are determined statistically based on 69 specimens which failed in the pull-out limit state. For the fasteners used in this study, the $\alpha_1$ values are 0.71, 0.70, and 0.66 for the HILTI ENP2K-20L15, HILTI ENP-19L15, and RAMSET SBR9 fasteners, respectively. The $\alpha_2$ coefficients are set to unity for the HILTI ENP-19L15 and the RAMSET SBR9 fasteners because these types have knurling pattern on the shank and the point. Meanwhile, $\alpha_2$ value of the HILTI ENP2K-20L15 fastener is set to 0.55 to account for the lack of knurling pattern on the PAF point. For the $\alpha_3$ coefficient, it is revealed that it has an inverse proportion with the ratio of the embedded area of the fastener point ($A_2$) over the total area of the fastener point ($A_{\text{point}}$). The results of pull-out prediction are set out in Table 3 with the values of $\alpha_3$ which was determined for each fastener type using the equations in the Figure 7. The proposed model can conservatively predict the pull-out strength for most of the specimen groups with an average ratio of tested-to-predicted strength of 1.02 and an acceptable COV of 12%.

Table 3. The predictions of pull-out strength

| Specimen | $N_{\text{shank}}$ (kN) | $N_{\text{point}}$ (kN) | $N_{\text{react}}$ (kN) | $N_{\text{not}}$ (kN) | $N_{\text{test}}$ (kN) | $\frac{N_{\text{test}}}{N_{\text{not}}}$ |
|---|---|---|---|---|---|---|
| 3.7-2.4-3.0 | 8.32 | 0.00 | 0.00 | 8.32 | 8.32 | 1.00 |
| 3.7-2.4-4.0 | 9.89 | 0.00 | 0.00 | 9.89 | 10.77 | 1.09 |
| 3.7-3.0-4.0 | 9.89 | 0.00 | 0.00 | 9.89 | 11.48 | 1.16 |
| 3.7-2.4-6.0 | 18.75 | 0.17 | 2.22 | 16.70 | 16.78 | 1.00 |
| 3.7-3.0-6.0 | 16.84 | 1.16 | 4.64 | 13.36 | 13.76 | 1.03 |
| 3.7-4.0-6.0 | 13.66 | 2.59 | 6.35 | 9.91 | 10.46 | 1.06 |
| 4.5-2.4-3.0 | 9.89 | 0.00 | 0.00 | 9.89 | 9.89 | 1.00 |
| 4.5-2.4-4.0 | 11.74 | 0.00 | 0.00 | 11.74 | 13.13 | 1.12 |
| 4.5-3.0-4.0 | 11.74 | 0.00 | 0.00 | 11.74 | 12.61 | 1.07 |
| 4.5-2.4-6.0 | 16.61 | 5.23 | 7.14 | 14.70 | 14.73 | 1.00 |
| 4.5-3.0-6.0 | 14.34 | 6.78 | 8.06 | 13.06 | 13.10 | 1.00 |
| 4.5-4.0-6.0 | 10.57 | 8.86 | 9.14 | 10.28 | 12.25 | 1.19 |
| 4.5-2.4-9.0 | 17.96 | 11.58 | 10.72 | 18.81 | 13.93 | 0.74 |
| 4.5-3.0-9.0 | 15.51 | 12.03 | 10.92 | 16.62 | 12.05 | 0.73 |
| 4.5-4.0-9.0 | 11.43 | 12.24 | 11.01 | 12.66 | 10.30 | 0.81 |
| 4.5-3.0-20.0 | 10.53 | 8.31 | 5.97 | 12.87 | 16.03 | 1.25 |
| 4.0-1.5-3.0 | 8.30 | 0.00 | 0.00 | 8.30 | 8.30 | 1.00 |
| 4.0-2.4-3.0 | 8.30 | 0.00 | 0.00 | 8.30 | 8.46 | 1.02 |
| 4.0-1.5-4.0 | 9.86 | 0.00 | 0.00 | 9.86 | 10.70 | 1.09 |
| 4.0-1.5-6.0 | 17.43 | 1.52 | 7.16 | 11.79 | 11.53 | 0.98 |
| 4.0-2.4-6.0 | 14.58 | 3.92 | 7.39 | 11.11 | 11.78 | 1.06 |
| 4.0-3.0-6.0 | 12.68 | 5.29 | 7.46 | 10.50 | 10.48 | 1.00 |
| 4.0-4.0-6.0 | 9.51 | 7.13 | 7.54 | 9.10 | 8.68 | 0.95 |
| | | | | | **Mean** | **1.02** |
| | | | | | **COV** | **0.12** |

The accuracy of the proposed model can also be justified based on the prediction for a larger test database which was collected from a study of Beck et al. [12]. The fastener used in their test series was the HILTI ENP-19L15 fastener which was identical to the one used in this paper (as illustrated in Figure 1). Therefore, it is reasonable to use the previously determined values of $\alpha_1$, $\alpha_2$, and $\alpha_3$ for the prediction. In the Beck et al. study, the base steel material had the thickness of 20 mm and the characteristic tensile strength of 400 MPa, from which the nominal yield strength and tensile strength is assumed to be 299 MPa and 478 MPa, respectively. The

results of the prediction is illustrated in Figure 8 as a relationship between pull-out strength and the embedment length. It can be seen that when the embedment length is insufficient ($l_e \leq 6.0$ mm), only the holding strength at the fastener point, $N_{point}$, develops. However, it is negated by the reactionary force, $N_{react}$, and eventually results in no holding strength. When $l_e > 6.0$ mm, the holding strength along the fastener shank, $N_{shank}$, starts to develop and keeps increasing when the penetration length increases. This component gradually becomes the primary force which holds the fastener in the base material because the holding force at the point cannot increase further when the entire point has been already embedded. The final $N_{not}$ prediction using this model produces a reasonable lower bound to most of the test data.

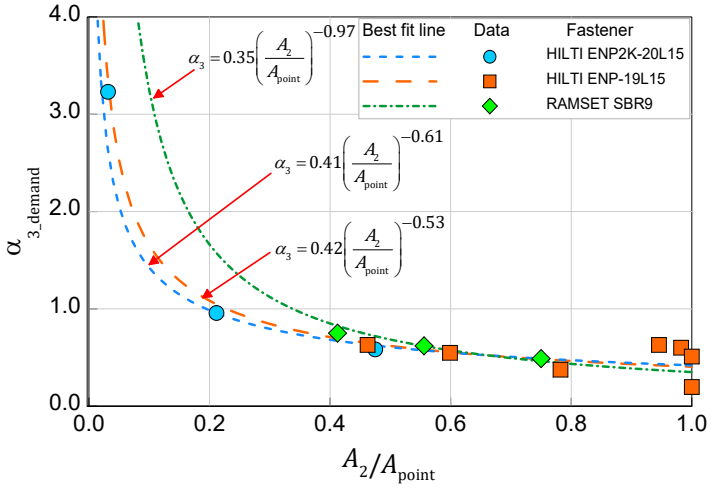


Figure 7. Determination of $\alpha_3$ coefficient

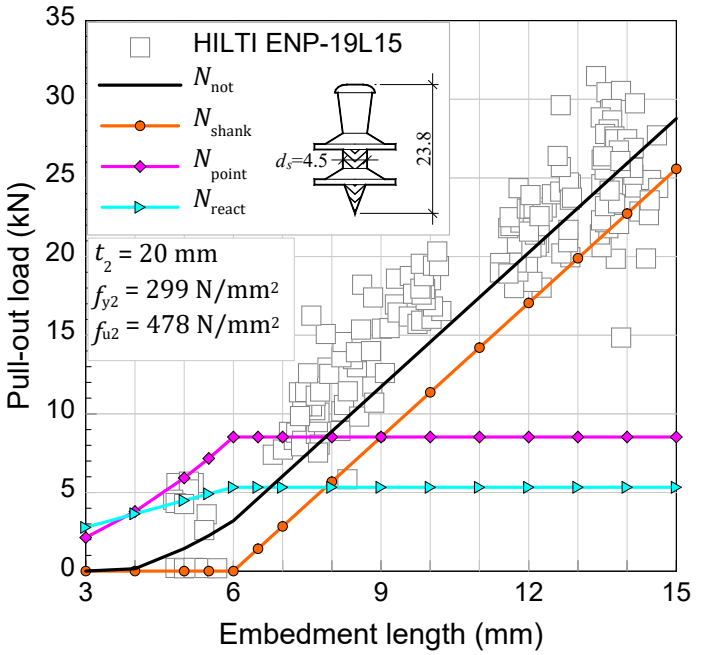


Figure 8. Prediction for Beck et al. [12] test database using the proposed model

## 5. Conclusions

This paper presents 69 cross-tension tests to investigate the pull-out limit state of Power-Actuated Fastener in cold-formed steel connections subjected to tension. Based on the test results, a model is proposed to evaluate the pull-out capacity by using the embedment length, the properties of the base steel material, and the geometric features of the fastener. To consider the diversity of the commercially available PAF, the prediction model utilizes a set of three coefficients $\alpha_1$, $\alpha_2$, and $\alpha_3$ which are calibrated from the experimental results. The proposed model is able to predict accurately the average ratio of tested-to-predicted pull-out strength of 1.02 with an acceptable COV of 12% for the tested specimens using three type of fasteners i.e. HILTI ENP2K-20L15, HILTI ENP-19L15, and RAMSET SBR9. For the other types of PAFs with different configurations in terms of geometry, knurling, metallurgical properties, the values of $\alpha_1$, $\alpha_2$, and $\alpha_3$, should be re-determined through statistical studies by the researchers or the manufacturers and can then be passed to the engineers for design.

## 6. Acknowledgements

This research was funded by the Australian Research Council Discovery Project through the Grant ID DP160104640. The first author's research degree was supported by the Dean's Faculty of Engineering and Information Technologies PhD Scholarship for Vietnam, the University of Sydney. The steel sheets were provided by BlueScope Steel. The HILTI power-actuator tool, fasteners and charges were provided by Hilti Pty Ltd.

## References

[1] AISI S100-16, North American Specification for the Design of Cold-Formed Steel Structural Members. Washington, DC, U.S.A., AISI, 2016.

[2] AS/NZS 4600:2018, Cold-formed steel structures. Sydney, Australia. Standards Australia, 2018.

[3] Mujagic, J., P. S. Green and W. G. Gould, Strength Prediction Model for Power Actuated Fasteners Connecting Steel Members in Tension and Shear - North American Applications. In Proc., 20th Int. Specialty Conf. on Cold-Formed Steel Structures. Missouri University of Science and Technology, Rolla, MO, U.S.A. 2010.

[4] Hilti Corporation, Direct Fastening Technology Manual 2018, Liechtenstein. 2018

[5] ITW Ramset Australia Pty. Ltd., SBR9 Technical Data. Victoria, Australia. 2007.

[6] Kosteski, N., J. A. Packer and M. Lecce, Nailed tubular connections under fatigue loading. Journal of Structural Engineering 126(11): 1258-1267, 2000.

[7] Fontana, M. and H. Beck, Experimental studies on novel shear rib connectors with powder-actuated fasteners. Composite Construction in Steel and Concrete IV, American Society of Civil Engineers, 426-437, Reston, VA, U.S.A., 2002.

[8] Rogers, C. A. and R. Tremblay, Inelastic seismic response of frame fasteners for steel roof deck diaphragms. Journal of Structural Engineering 129(12): 1647-1657, 2003.

[9] AS 1397:2011, Continuous hot-dip metallic coated steel sheet and strip - Coatings of zinc and zinc alloyed with aluminum and magnesium. Sydney, Australia. Standards Australia, 2011.

[10] AS/NZS 1163:2016, old-formed structural steel hollow sections. Sydney, Australia. Standards Australia, 2016.

[11] AS/NZS 3678:2016, Structural steel - Hot-rolled plates, floorplates and slabs. Sydney, Australia. Standards Australia, 2016.

[12] Beck, H., M. Siemers and M. Reuter, Stahlbau kalender. Berlin, Germany. Ernst & Sohn, 2011.